Food Chemistry: X 21 (2024) 101229

Contents lists available at ScienceDirect

Food Chemistry: X

journal homepage: www.sciencedirect.com/journal/food-chemistry-x

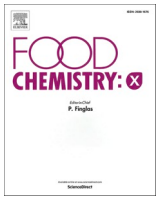

Effect of sanxan on the composition and structure properties of gluten in salt-free frozen-cooked noodles during freeze–thaw cycles

Ying Liang [a], Xiuling Zhu [a], Hao Liu [a], Jiayi Wang [a], Baoshan He [b], Jinshui Wang [a,*]

[a] College of Biological Engineering, Henan University of Technology, Zhengzhou 450001, China
[b] College of Food Science and Engineering, Henan University of Technology, Zhengzhou 450001, China

ARTICLE INFO

Keywords:
Sanxan
Salt-free frozen-cooked noodles
Gluten
Freeze–thaw cycles
Conformational change

ABSTRACT

In this study, the mechanisms by which sanxan protected the quality of salt-free frozen-cooked noodles (SFFCNs) were investigated, with a focus on the composition and structural properties of gluten. The results showed that sanxan facilitated the formation of glutenin macropolymer and maintained the stabilization of glutenin subunits in freeze–thaw cycles (FTs). In terms of protein structure, sanxan weakened the disruption of secondary structure caused by FTs and increased the proportion of *gauche-gauche*-gauche (g-g-g) conformations in the disulfide (S—S) bonds bridge conformation. Simultaneously, sanxan reduced the exposure degree of tryptophan (Trp) and tyrosine (Tyr) residues on the protein surface. Moreover, the intermolecular interaction forces indicated that sanxan inhibited S—S bonds breakage and enhanced the intermolecular crosslinking of gluten through ion interactions, which was crucial for improving the stability of gluten. This study provides a more comprehensive theoretical basis for the role of sanxan in improving the quality of SFFCNs.

1. Introduction

With the improvement of people's living standards, noodles have gradually evolved to become more convenient, nutritious, and with optimal and diverse flavors. Frozen cooked noodles (FCNs) are a new type of convenient noodles product developed in recent years. They consist of cooked noodles that have been cooled and frozen quickly for long-term storage and can be consumed after briefly reheated (about 90 s) (Obadi, Zhang, Shi, & Xu, 2021). The addition of NaCl has been reported to affect the rheological properties of dough by improving non-covalent gluten cross-linking, competing for water absorption, reducing protein solubility by covering polar groups and strengthening the structure of the gluten network (Reissner, Wendt, Zahn, & Rohm, 2019). The addition of NaCl facilitates the aggregation of gliadin and glutenin through intermolecular hydrogen bonding or ionic bonding, facilitating the cross-linking of more proteins to form a tightly networked structure, thereby reducing the adverse effects of frozen storage on the quality of FCNs (Ukai, Matsumura, & Urade, 2008). However, excessive salt intake can have adverse impacts on an individual's well-being.

In recent years, there has been an increasing focus on health issues related to high salt intake, including hypertension, cardiovascular disease, and strokes (Chen, Hu, & Li, 2018). The Dietary Guidelines for Chinese Residents (2022) stipulate that daily salt intake for adults should not exceed 5 g; however, the salt consumption per capita in China (9.3 g/d) far exceeds this recommended limit. Therefore, it is crucial to reduce salt intake in China, and the development of salt-free frozen-cooked noodles (SFFCNs) holds great promise. However, the lack of NaCl affects gluten hydration at the kneading stage, resulting in differences in the gluten microstructure and changes in the molecular conformation and network structure. As a result, it impacts the physicochemical properties of the dough, ultimately reducing the quality of the FCNs, particularly affecting gluten and its network structure. How to eliminate the effects of NaCl deficiency on gluten and its network structure is the key to improving the quality of SFFCNs.

The addition of modifiers is one of the strategies to improve the quality of FCNs. Among them, hydrophilic colloid is a better modifier for quality improvement. Enhancements in FCNs quality were observed when hydrophilic colloids such as xanthan, curdlan, guar gum, and pullulan were incorporated (Hong et al., 2021; Liang et al., 2020; Obadi et al., 2021; Pan, Ai, Wang, Wang, & Zhang, 2016). Among them, curdlan has the characteristics of heating glue, which can reduce the deterioration of the quality of FCNs during freezing storage by affecting the denaturing behavior of gluten and the rearrangement behavior of

* Corresponding author.
E-mail address: jinshuiw@163.com (J. Wang).

https://doi.org/10.1016/j.fochx.2024.101229
Received 3 November 2023; Received in revised form 1 February 2024; Accepted 12 February 2024
Available online 15 February 2024

the structure of the gluten network during the maturation process (Liang et al., 2022). Xanthan, guar gum, and pullulan have gelling properties of cold water that remain unchanged after heating and are used to influence the hydration of gluten and the formation of gluten networks during the preparation of raw noodles, thus affecting the overall quality of FCNs. However, the factors that caused the deterioration of FCNs frozen storage quality were the two stages of raw noodles cooking and making. The formation and rearrangement of the structure of the gluten network and the hydration and denaturation of gluten were the key factors that affected the degree of gluten depolymerization and the quality of FCNs during frozen storage. Therefore, how to control the two stages at the same time is the most efficient way to slow the degradation of the quality of FCNs during frozen storage. Unlike other colloids, sanxan exhibits shear-thinning properties at high temperatures and also forms gels with good freeze–thaw stability at low temperatures (Wu et al., 2017). Based on this, the cross-linking aggregation of gluten inside the noodles is not hindered during the cooking process of SFFCNs. Moreover, during low-temperature storage, sanxan can effectively restrict the flow of water and thus inhibit the formation of ice crystals, which improves the resistance and stability of SFFCNs. Therefore, we believe that sanxan can affect gluten and its network structure during the production and cooking stages of raw noodles from SFFCNs, to attenuate quality deterioration in the freeze–thaw cycles (FTs), and is considered an efficient quality improver for SFFCNs. On the basis of the gel characteristics of sanxan, we established the multistage regulation technique for the quality of FCNs in the previous study and explored the effect on quality during FTs. However, it is not yet clear how sanxan affects gluten and its network structure in SFFCNs; so far, no relevant reports have been found. The unfolding and cross-linking of gluten form a dense network structure, which can enhance the shape and texture properties of salt-free FCNs. Therefore, it is important to study the effect of sanxan on gluten and its network to elucidate the potential mechanism of sanxan to improve the quality of SFFCNs during FTs.

According to the results of our previous experiments, the addition of 1.2 % sanxan was found to have the best modification effect on SFFCNs, but its effect on the composition and structural properties of gluten in SFFCNs has not been systematically analyzed (Liang et al., 2023). Therefore, the main objective of this study was to investigate in depth the cryoprotective effect of the addition of sanxan on SFFCNs, focusing on the effect of sanxan on the composition and structural properties of the gluten of SFFCNs during FTs. The molecular weight distribution and the subunit distribution of gluten mediated by the addition of 1.2 % sanxan were systematically investigated (Sodium dodecyl sulphate–polyacrylamide gel electrophoresis (SDS-PAGE) and reversed-phase high-performance liquid chromatography (RP-HPLC)); secondary and tertiary structural changes were elucidated by using Fourier-transform infrared (FT-IR) spectroscopy and Raman spectroscopy; and covalent bonding, non-covalent bonding, and interaction forces between surface hydrophobic molecules were explored. This study provides a more comprehensive theoretical basis for the fortification effect of sanxan on the improvement of the quality of SFFCNs from the perspective of gluten, contributing to enhancing their overall quality.

2. Materials and methods

2.1. Materials

The sanxan sample (Purity > 99 %), with a molecular weight of 408 kDa and a polydispersity index (Mw/Mn) of 1.07, was purchased from Xinhe Biochemical CO., Ltd., Hebei, China. The Zhongliang Flour Industry Co., Ltd. provided wheat flour (with a moisture content of 12.70 %, an ash content of 0.35 %, and a protein content of 13.20 %) (Zhengzhou, China) for the study. Except for the chemicals mentioned above, all experimental substances were of analytical grade quality.

2.2. Preparation of SFFCNs

The procedures used to prepare SFFCNs were consistent with the methodology outlined in our previous research (Liang et al., 2020). Mix 100 g of flour with 0 g (control group) and 1.2 g (experimental group) of sanxan (w/w, on flour basis) evenly, then add it to a dough mixer (JHMZ200, East Fude Technology Development Center, Beijing, China) along with 40 g of distilled water. Mix and knead the dough for 7 min, then securely cover it with plastic wrap. Allow the dough to rest at room temperature for a period of 20 min. Finally, use a noodles machine (JMTD-168/140, Beijing Dongfu Jiuheng Instrument Technology Co., Ltd., Beijing, China, and dia 10.0 mm) to cut it into noodles with a width of 2.00 mm. Take 30.0 g of the noodles mentioned above and cook them in 300 mL of boiling water for 7 min, then remove and drain. Subsequently, the noodles were first frozen at −50 °C for 2 h, followed by further freezing at −18 °C for 46 h before being removed and thawed at room temperature for 2 h, which was a FT of 0 (frozen for 2 h), 2, 4, 6, 8 and 10 FTs. Subsequently, the noodles were subjected to a freeze-drying process and subsequently pulverized for further analysis and determination.

2.3. Sodium dodecyl sulphate - polyacrylamide gel electrophoresis (SDS-PAGE)

According to the method of Wang, Liang, Wang, Zhang, and Wang (2021), SDS-PAGE electrophoresis was performed to analyze alterations in the distribution of gluten molecular weight within SFFCNs and appropriate adjustments were implemented. The SFFCNs sample (100 mg) was dispersed in 1.0 mL of Tris-HCl buffer (0.0625 mol/L, pH 6.8, 20 % glycerol, 2.0 % SDS, 0.1 % bromophenol blue). For further analysis, the supernatant was obtained by extracting samples for 3 h through agitation at 25 °C (200 r/min), followed by heating in a boiling water bath for 5 min and centrifugation at 10,000 r/min for 10 min. 5 % β-mercaptoethanol should be added to the above buffer for SDS-PAGE under the reduction condition. The treated sample (10 μL) was injected into the swim lane of a vertical electrophoresis plate containing a 10 % separation gel concentration (pH 8.8) and 5 % concentrated gel (pH 6.8). At a steady 100 V voltage, electrophoresis ceased when the bromophenol blue indicator reached the bottom of the separation gel and the gel was taken out. After a 1 h staining period with Coomassie bright blue dye, the gel was then transferred to the solution for decolorization.

2.4. Revered-phase high-performance liquid chromatography (RP-HPLC)

According to the method of Wang, Guo, and Zhu (2016), SFFCN samples were processed. The 200 mg samples were accurately weighed and extracted twice with 3 mL of phosphate buffer solution (0.05 mol/L, pH 7.6, containing 0.4 mol/L sodium chloride) and the supernatant was discarded. Then extract with 3 mL of deionized water twice, discarding the supernatant; the precipitation was extracted with 3 mL of 60 % (v/v) ethanol three times and the supernatant was collected after centrifugation (10000 r/min). The precipitation was further extracted with Tris-HCl buffer solution (0.05 mol /L, pH 7.5, containing 50 % (v/v) isopropyl alcohol, 2 mol/L urea, 0.1 % (w/v) dithiothreitol (DTT)) three times, 3 mL each time. After centrifugation (10000 r/min), the supernatant was collected to form the glutenin extraction solution. The gliadin and glutenin extracts were filtered by 0.45 μm filtration membrane, respectively. Agilent HPLC was used to analyze the extract of SFFCN samples. Nucleosil 300–5 C8 (250 × 4.6 mm), mobile phase: acetonitrile containing 0.1 % (v/v) trifluoroacetic acid and water containing 0.1 % (v/v) trifluoroacetic acid, elution conditions: gradient elution (acetonitrile concentration increased from 24 % to 56 % (0–50 min), 56 % to 24 % (50–60 min), flow rate is 1 mL per minute, column temperature is set at 50 °C, and wavelength used for detection is 214 nm. The gluten subunits were separated by different retention times during elution as a result of their varying polarities. Reference was made to the

method of Wieser, Antes and Seilmeier (1998) to differentiate the subunits, and then the change in content was estimated based on the peak area corresponding to each subunit.

2.5. Fourier transform infrared (FTIR) spectroscopy

A Fourier infrared spectrometer was employed to assess the secondary structure of the SFFCNs. According to the method proposed by Zhang, Ma, Yang, Li, and Sun (2022b), the freeze-dried SFFCNs sample was homogeneously mixed with potassium bromide in a 1:100 (w/w), and then thoroughly ground using an agate mortar before being pressed into transparent rounds. Potassium bromide was used as the background to scan the infrared spectrum of the sample. The spectrum scanning range was 400–4000 cm^{-1}, with a total of 16 scans conducted and a resolution set at 4 cm^{-1}. The spectra of amide I at 1650–1659 cm^{-1}, 1610–1640 cm^{-1}, 1660–1700 cm^{-1} and 1640–1650 cm^{-1} were α-helix, β-sheet, β-turn and random coil, respectively. Quantification of the secondary structure content involves determining the proportion between the area of the amide I region and the total area. The spectral analysis was carried out using the software Peakfit v4.12.

2.6. Fourier transform (FT)-Raman spectroscopy

The conformation of disulfide bonds and aromatic amino acid SFFCNs was analyzed using confocal Raman spectroscopy (RFT-6000FT, JASCO, Europe) (Wang et al., 2020). The spectra were acquired within the range of 400–3500 cm^{-1} using a 1064 nm laser with a resolution of 1 cm^{-1}. Baseline correction was performed using Origin v8.0 (Origin Lab Inc., MA, USA), followed by normalization based on the peak phenylalanine at 1003 cm^{-1}. Raman spectra before and after normalization (Fig. S2). The spectral region ranging from 490 to 560 cm^{-1} was subjected to S—S conformation analysis using Peak-fit 4.12 software (Systat Software, Chicago, USA) with the application of deconvolution techniques.

2.7. Free sulfhydryl (SH) and disulfide (S—S) bonds ratio

The method used to determine the levels of free sulfhydryl (SH) and disulfide (S—S) bonds in the SFFCNs was based on the method of Wang, Zhang, Xu, and Li (2020) with some adjustments made for our specific study.

In brief, the lyophilized sample (75 mg) was dissolved in 1.0 mL of Tris-Gly buffer (86 mmol/L, pH 8.0), which contained 10.4 g/L Tris, 6.9 g/L glycine, and 12.0 g/L EDTA. Subsequently, guanidine hydrochloride (4.7 g) was added to the solution, followed by fixing the volume at 10 mL with the same Tris-Gly buffer and stirring for 3 h at a temperature of 25 °C and a speed of 150 rpm while vortexing for one minute every half hour interval. Finally, centrifugation was performed at a speed of 10,000 r/min for 10 min to obtain the supernatant.

The determination of the total SH content involved mixing 1 mL of supernatant with a solution consisting of 4 mL of urea-guanidine hydrochloride (prepared by dissolving 4.8 g of each urea and guanidine hydrochloride in 10 mL of Tris-glycine buffer containing 0.05 % β-mercaptoethanol mixture) was stirred at a temperature of 25 °C for a duration of 3 h. Subsequently, to the mixture, 10 mL of trichloroacetic acid (13 %) was added and allowed to stand for an hour in an incubator set at a temperature. After centrifugation (9000 r/min, for a period of 10 min), the resulting supernatant was discarded and two washes were performed using each time a 5 mL solution of urea trichloroacetic acid. To dissolve the precipitate, we used a solution containing 10 mL of urea (8 mol/L). Finally, Ellman's reagent (DTNB) was introduced by precisely adding 0.04 mL to the dissolved precipitate followed by measuring its absorbance at wavelength A_{412}. The total SH content (μmol/g) was calculated using Eq. (1).

The determination of the free SH content was performed by mixing 1 mL of supernatant with 4 mL of a solution of urea-guanidine hydrochloride (prepared by dissolving 4.8 g of each urea and guanidine hydrochloride in 10 mL of Tris-glycine buffer) and adding 0.05 mL of Ellman's reagent (DTNB, 4 mg/mL). The absorbance at 412 nm (A_{412}) was then measured. Free SH content (μmol/g), S—S bonds content (μmol/g), and free SH to S—S bonds ratio were calculated using Eq. (2) , Eq. (3), and Eq. (4), respectively.

$$\text{Total SH content} = 73.53 \times A_{412} \times \frac{D}{C} \quad (1)$$

$$\text{Free SH content} = 73.53 \times A_{412} \times \frac{D}{C} \quad (2)$$

$$\text{S - S bonds content} = \frac{\text{total SH content} - \text{free SH content}}{2} \quad (3)$$

$$\text{Free SH and S - S bonds ratio} = \frac{\text{free SH content}}{\text{S - S bonds content}} \quad (4)$$

where D and C denote the dilution factor and the sample concentration (mg/mL), respectively.

2.8. Determination of chemical interactions

The determination of the non-covalent bond interaction forces was slightly modified according to the method of Wang, Luo, Zhong, Cai, Jiang, and Zheng (2017). Based on 0.05 mol/L phosphate buffer (pH 7.0), the following solutions were prepared: 0.05 mol/L NaCl (S1), 0.6 mol/L NaCl (S2), 0.6 mol/L of NaCl + 1.5 mol/L of urea (S3), and 0.6 mol/L of NaCl + 8 mol/L of urea (S4). Freeze-dried samples of SFFCNs (200 mg) were dissolved in 10 mL of four solutions, shaken (200 r/min, 25 °C) for 3 h, centrifuged (10,000 r/min, 10 min). Quantification of protein concentration in the supernatant was performed using the Coomassie brilliant blue technique, where bovine serum albumin served as the standard reference. The concentration of soluble protein was measured as mg/mL.

2.9. Determination of surface hydrophobicity

The surface hydrophobicity was determined using the bromophenol blue (BPB) method with appropriate modifications (Tang et al., 2019). The sample (50 mg) was thoroughly mixed with 1 mL of a sodium phosphate buffer (pH 7.0) at a concentration of 20 mmol/L, followed by the addition of 200 μL of BPB solution (1 mg/mL). The mixture was then gently oscillated at a speed of 200 r/min and maintained at a temperature of 25 °C for a duration of 1 h. After centrifugation (4000 r/min, 10 min), 100 μL of supernatant was aspirated and 900 μL of sodium phosphate buffer was added. The absorbance was measured by an ultraviolet spectrophotometer at 595 nm, zeroed with phosphate buffer, and the solution without sample was used as a blank control. Surface hydrophobicity was quantified on the basis of the fixation of BPB with non-soluble proteins and binding of BPB. The amount of BPB binding (μg) was given by Eq. (5):

$$\text{BPB binding} = \frac{\left(A_{\text{control}} - A_{\text{experimental}}\right)}{A_{\text{control}}} \times 2 \times 10^{-4} \quad (5)$$

Where A is the absorbance at 595 nm.

2.10. Statistical analysis

All data were presented as mean ± standard deviation of at least three independent experiments and were subjected to statistical analysis using SPSS software (version 13.0 for Windows, SPSS Inc., Chicago, IL). The significance of the differences was assessed by a one-way analysis of variance (ANOVA) with the Tukey post hoc test. A significance level $P < 0.05$ was considered to indicate a statistically significant degree of variation. Each experiment involved measurements in triplicate.

3. Results and discussion

3.1. Effect of sanxan on the change of molecular weight of gluten in SFFCNs during FTs

The effects of sanxan on the relative molecular weight of gluten in SFFCNs were analyzed by SDS-PAGE, as shown in Fig. 1.

In gel electrophoresis, there is an inverse relationship between the migration rate of protein subunits and their relative molecular weights (Wang, Wu, Rasoamandrary, Jin, & Xu, 2015). Under non-reducing conditions (Fig. 1A), during FTs, the strength of the band corresponding to 180 kDa in the control group was weakened, indicating that FTs would cause depolymerization of aggregates. Liu et al. (2024) also reached a similar conclusion that depolymerization of aggregates occurs during freezing and storage. However, the intensity of the aggregate bands was significantly increased with the addition of sanxan. This suggests that sanxan was beneficial in maintaining structural stability during FTs, even after 10 FTs, it remained similar to the control group with 0 FT. This indicates that gluten formed more aggregates at an early stage, and sanxan had a favorable effect on the aggregation of gluten during the cooking stage. These results indicate that sanxan had a certain inhibitory effect on the formation of cross-links between SDS-insoluble macromolecules and their entanglement with SDS-soluble proteins. The absence of sulfhydryl groups in both ω-gliadin and α/β-gliadin prevents them from polymerization through disulfide bonds (Wang et al., 2014; Wang et al., 2016). This may contain two potential mechanisms: one is that the interaction between sanxan and gluten directly strengthens the gluten matrix, while the other is that sanxan inhibits water mobility, reducing ice crystal formation and thereby preventing destruction of gluten by ice crystals (Li et al., 2022). Thus, sanxan promoted the formation of aggregates to some extent through some non-covalent interactions. In the HMW-GS and low to medium-molecular weight range, the intensity of the bands did not vary significantly between lanes. When the sample was treated with a reducing agent (β-mercaptoethanol), a portion of the highly aggregated protein could be extracted once again. Under the reduction condition (Fig. 1B), it could be observed that there were no significant alterations in both the quantity and intensity of the protein bands, suggesting that the addition of sanxan and frozen storage did not exert any impact on the reduced protein subunits.

3.2. Effect of sanxan on changes in the gluten subunit in SFFCNs during FTs

According to the polarity difference of the gluten subunits, the gluten subunits were separated by reverse-phase high-performance liquid chromatography. The distribution of protein subunits is shown in Fig. 2A and C (gliadin subunits) and 2B and D (glutenin subunits). Fig. S1 illustrates the proportions of the gliadin and glutenin subunits and the percentages of total gliadin and total glutenin. The subunits of gliadin can be classified into three groups: sulfur-poor ω- gliadin, sulfur-rich α- and γ- gliadin; glutenin subunits can be classified into four main types: high molecular weight glutenin subunits (HMS) and low molecular weight glutenin subunits (B/C-LMS and D-LMS) (Aghagholizadeh et al., 2017).

As the number of FTs increased, the relative content of D-LMS in the control group appeared to increase, the content of γ-gliadin subunits decreased, and the content of the HMS, B/C-LMS, α-, ω1,2- and ω5-gliadin subunits did not change significantly. However, compared to the control group, the percentage of D-LMS in the SFFCNs in the experimental group decreased, while the content of γ -gliadin subunit increased. As shown in Fig. S1, with the increase in the number of FTs, the glutenin content gradually increased from 69.76 to 77.46 (control group) and 60.22 to 71.86 (experimental group), while gliadin decreased from 30.27 to 22.54 (control group) and 39.78 to 28.14 (experimental group). Compared to the control group, samples containing 1.2 % sanxan exhibited a significant reduction in gliadin content under identical FTs. During FTs, gluten was significantly affected by the water phase transition, particularly in terms of ice crystal formation and recrystallization. Therefore, the presence of ice crystals caused significant degradation of the cross-linking network of disulfide bonds within the gluten system due to mechanical damage. Combined with SDS-PAGE, it was found that the content of glutenin increased as FTs increased in the presence of sanxan. This could be attributed to an increase in the total amount of gluten monomers resulting from depolymerization of glutenin macropolymer. Additionally, sanxan helped maintain stability of gluten subunits within FTs. Compared to the control group, the presence of sanxan, promoted the formation of intramolecular disulfide bonds among glutenin subunits. Glutenin participated in the polymerization, which led to a decrease in the extraction rate.

3.3. Effect of sanxan on the secondary structure of gluten in SFFCNs during FTs

The conformational change of gluten, which plays a crucial role in the formation of its network structure, is directly indicated by its secondary structure (Li, Sun, Han, Chen, & Tang, 2018). Among the nine distinctive absorption bands, the amide I region (1700–1600 cm^{-1}) demonstrates the highest sensitivity to discerning the secondary conformation of proteins. Table 1 presents the alterations in the secondary structure content of gluten within SFFCNs treated with sanxan compared to the control group during FTs.

With increasing FTs, the content of α-helices in the control group

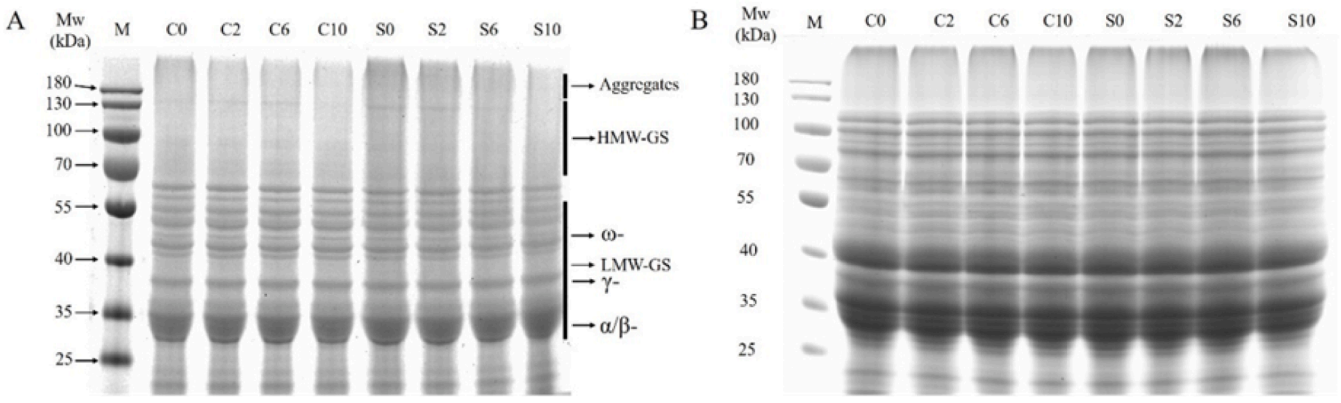

Fig. 1. SDS-PAGE images of gluten in SFFCNs under non-reduced (A) and reduced (B) conditions. Note: C: Without sanxan addition; S: Sanxan addition 1.2 %; 0, 2, 6, and 10 represent the number of FTs, respectively. Abbreviations are: SFFCNs, salt-free frozen-cooked noodles. FTs: freeze–thaw cycles.

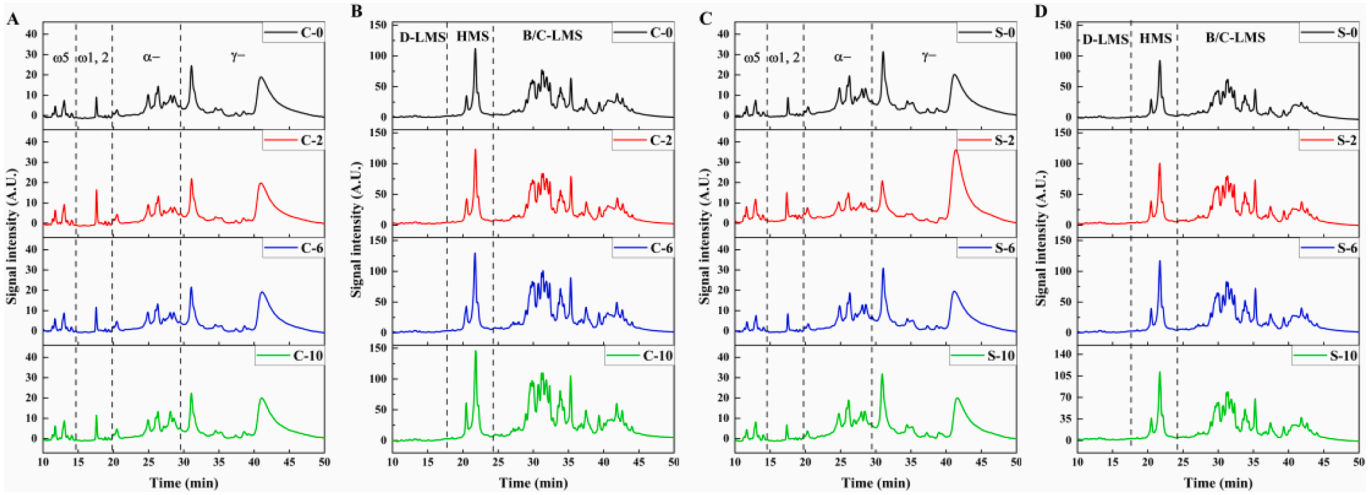

Fig. 2. Reversed-Phase HPLC chromatogram of gliadin (A, C) and glutenin (B, D) subunits extracted from SFFCNs with 1.2 % (C, D) and without (A, B) sanxan. Note: C: Without sanxan addition; S: Sanxan addition 1.2 %; 0, 2, 6, and10 represent the number of FTs, respectively. Abbreviations are: SFFCNs, salt-free frozen-cooked noodles. FTs: freeze–thaw cycles.

Table 1
Effect of sanxan on the secondary structure of gluten of SFFCNs during FTs.

Sanxan (%)	FT (cycles)	Secondary structures (%)			
		α-Helices	β-Sheets	β-Turns	Random coils
0	0	15.45 ± 0.24^{aA}	25.06 ± 0.36^{cB}	40.30 ± 0.35^{aA}	19.19 ± 0.23^{cA}
	2	12.03 ± 0.01^{bA}	28.27 ± 0.33^{aA}	40.26 ± 1.16^{aA}	20.45 ± 0.84^{cA}
	6	10.94 ± 0.36^{bA}	26.60 ± 0.34^{bA}	37.87 ± 1.22^{abA}	24.59 ± 0.52^{bA}
	10	10.74 ± 0.21^{bA}	27.68 ± 0.13^{abA}	35.26 ± 1.06^{bA}	26.53 ± 0.33^{aA}
1.2	0	16.16 ± 0.60^{aA}	23.95 ± 0.14^{aA}	40.70 ± 0.32^{aA}	19.19 ± 0.42^{aA}
	2	15.58 ± 0.36^{aB}	26.23 ± 1.13^{aA}	40.93 ± 0.51^{aA}	17.26 ± 0.62^{bB}
	6	15.22 ± 0.00^{aB}	25.40 ± 0.40^{aA}	40.47 ± 0.21^{aA}	18.90 ± 0.51^{abB}
	10	15.03 ± 0.18^{aB}	24.97 ± 1.09^{aA}	39.77 ± 0.72^{aA}	20.23 ± 0.19^{aB}

Note: Data are expressed as mean ± standard deviation (n = 3). Different lowercase letters indicated significant difference under the same dosage and different FTs ($P < 0.05$); Different capital letters indicated that sanxan had significant differences under different dosage and same FTs ($P < 0.05$). Abbreviations are: SFFCNs, salt-free frozen-cooked noodles. FTs: freeze–thaw cycles.

decreased significantly ($P < 0.05$), while the content of the random coil increased significantly. Since the α-helices structure is more ordered than other secondary structures (Georget & Belton, 2006), this suggests that gluten tends to be disordered. Hydrogen bonding plays a crucial role in maintaining the stability of the protein's secondary structure. With the increase in the number of FTs, temperature fluctuations cause water migration and recrystallization, leading to the destruction of hydrogen bonds in the protein structure. As a result, polypeptide chains tend to stretch, gradually exposing the hydrophilic and hydrophobic regions of proteins to new environments, resulting in new molecular cross-linking within and between protein molecules, thereby altering the secondary structure of proteins (Liang,et al., 2022).

With the addition of sanxan, the α-helices content decreased gradually but was significantly higher than that of the control group with the same FTs. The content of the random coil gradually increased with FTs, but was significantly lower than that in the same FTs control group. The change in β-turns was not significant. These results indicate that sanxan can reduce the damage of the gluten structure caused by ice crystals to a certain extent and stabilize the secondary structure of gluten during FTs. Comparable findings were discovered in the literature documented by Liang et al. (2022), α-helices increased after adding curdlan, suggesting that curdlan enhanced the hydrogen bond of gluten during frozen storage, thus stabilizing the secondary structure during frozen storage. In addition, the addition of sanxan enhanced the hydration of gluten and contributed to the formation of the protein-water bond in gluten. The increased ductility of protein molecules helps increase the chance of interaction between molecules, so each secondary structure in protein has a relatively stable state.

3.4. Effect of sanxan on conformation changes of disulfide (S—S) bond bridges of gluten in SFFCNs during FTs

The presence of S—S bonds plays a crucial role in the preservation of the tertiary conformation of the protein. The conformational change can be evaluated by measuring the S—S bonds stretching vibration (Wieser, 2007). The configuration of the carbon atom within the S—S bonds bridge significantly influences the symmetric stretching motion of the S—S bonds. Based on the distinct atomic arrangements of C—S—S—C, it is possible to classify the three configurations within the 490–550 cm^{-1} range: *gauche-gauche*-gauche (g-g-g) (510 cm^{-1}), *gauche*-gauche-trans (g-g-t) (525 cm^{-1}) and *trans*-gauche-trans (*t*-g-t) (540 cm^{-1}) (Brandt, Chikishev, Golovin, Kruzhilin, & Zalevsky, 2014).

As shown in Table 2, with the increase in the number of FTs, the g-g-g configuration content of the sample showed an increasing trend, and the g-g-g configuration content of the control group increased by 5.11 % (from 72.31 % to 77.42 %) and that of the experimental group increased by 3.96 % (from 72.78 % to 76.74 %). The content of the g-g-t conformation and the *t*-g-t conformation exhibited a notable decrease. The g-g-g conformation is the most stable structure, the lowest energy, and the least ductile (Zhou et al., 2014). Combined with the decrease in S—S bonds content, it is reasonable to speculate that the increase in g-g-g is due to the structural instability of the breaking of g-g-t and *t*-g-t in FTs. The presence of sanxan effectively prevents the breakdown of the g-g-t and *t*-g-t structures, thereby promoting the preservation of the stable structure of gluten and offering a protective effect in delaying gluten contraction.

Table 2
Effects of sanxan on the microenvironment of gluten amino acids and conformational changes of disulfide bond of SFFCNs during FTs.

Sanxan (%)	FT (cycles)	Aromatic amino acid environment		Disulfide bridges conformations		
		I_{755}	I_{854}/I_{830}	g-g-g (%)	*t*-g-g (%)	*t*-g-t (%)
0	0	0.24 ± 0.01^{cA}	4.21 ± 0.06^{cA}	72.31 ± 0.47^{cA}	21.51 ± 0.02^{aA}	6.18 ± 0.28^{aA}
	6	0.39 ± 0.03^{bA}	4.67 ± 0.08^{bA}	75.48 ± 0.55^{bA}	19.59 ± 0.07^{bA}	4.93 ± 0.53^{bA}
	10	0.51 ± 0.01^{aA}	5.25 ± 0.10^{aA}	77.42 ± 0.17^{aA}	18.44 ± 0.82^{cA}	4.14 ± 0.02^{cB}
1.2	0	0.21 ± 0.04^{aA}	4.16 ± 0.10^{bA}	72.78 ± 0.51^{bA}	21.08 ± 0.02^{aB}	6.14 ± 0.50^{aA}
	6	0.33 ± 0.01^{aA}	4.27 ± 0.04^{abB}	75.93 ± 0.15^{aA}	19.47 ± 0.37^{abA}	4.60 ± 0.22^{bB}
	10	0.40 ± 0.07^{aA}	4.68 ± 0.16^{aB}	76.74 ± 0.22^{aA}	18.56 ± 0.50^{bA}	4.70 ± 0.30^{bA}

Note: Data are expressed as mean ± standard deviation (n = 3). Different lowercase letters indicated significant difference under the same dosage and different FTs ($P < 0.05$); Different capital letters indicated that sanxan had significant differences under different dosage and same FTs ($P < 0.05$). Abbreviations are: SFFCNs, salt-free frozen-cooked noodles. FTs: freeze–thaw cycles.

3.5. Effect of sanxan on the micro-environment of aromatic amino acid of gluten in SFFCNs during FTs

The gluten structure was analyzed using Fourier transform Raman spectroscopy (FT-Raman), which facilitated the detection of changes in the conformational states of amino acids by examining the positions and intensities of the absorption peak (Wang et al., 2020). The alteration in the intensity of the 755 cm^{-1} band (I_{755}) can be used as a means to evaluate the strength of hydrogen bonds and to assess the level of exposure experienced by tryptophan (Trp) residues. Badii and Howell (2006) suggested that the decrease indicated a tendency for Trp residues to be located within a hydrophobic microenvironment, resulting in the formation of a more disordered structure. On the contrary, an increase in I_{755} indicated that Trp residues were exposed to a hydrophilic environment. As shown in Table 2, with an increase in the number of FTs, the value of I_{755} in the control group increased from 0.24 to 0.51, indicating that the hydrophobic polymerization of Trp residues was weakened when exposed to a hydrophilic environment. After the addition of 1.2 % sanxan, the I_{755} value increased from 0.21 to 0.40, and the change (0.19) was smaller than in the control group (0.27). This indicates that the presence of sanxan reduces the exposure of Trp residues, impedes the recrystallization of ice crystals in the FT process, and decreases the water's phase transition.

The presence of a bimodal ratio (I_{854}/I_{830}) in the vibrational frequencies of tyrosine (Tyr) at 854 and 830 cm^{-1} provides compelling evidence for the involvement of phenolic hydroxyl groups in hydrogen bonding. The decrease in I_{854}/I_{830} values corresponds to an increase in hydrogen bonding (Nawrocka et al., 2015). As shown in Table 2, the I_{854}/I_{830} ratio in the control group increased from 4.21 to 5.25 with the increase in FTs. This occurrence demonstrates the reduction in hydrogen bond content following FTs, which is further supported by the decrease in β-sheet content within the secondary structure. After adding 1.2 % sanxan, the I_{854}/I_{830} ratio increased from 4.16 to 4.68, and the change (0.52) was smaller than in the control group (1.04). This indicated that the addition of sanxan inhibited the reduction of hydrogen bonds in the FT process and the hydroxyl group in sanxan combined with gluten to form a hydrogen bond, which inhibited the overdevelopment of protein and delayed the depolymerization of gluten.

3.6. Effect of sanxan on the ratio of free sulfhydryl (SH) and disulfide (S—S) bonds of gluten in SFFCNs during FTs

As shown in Fig. 3A, the SH/S—S bonds ratio exhibited a significant increasing trend in the control group with the increase in the number of FTs, especially the number of 8, 10 times FTs increased significantly from 2.66 to 4.27. This indicated that the ice crystals were relatively active, causing relatively large damage to the proteins and showing a relatively high degree of depolymerization. During the FTs, the ratio of the experimental group also increased gradually but was always lower than that of the control group. These results indicated that the addition of sanxan could effectively inhibit the breakage of some S—S bonds, thus alleviating the depolymerization of gluten during the FTs. The 8, 10 times FTs in the addition of sanxan still maintained a low growth rate, indicating that sanxan inhibited the severe activity of the ice crystal. These results indicated that the partial S—S in the SFFCNs system broke with increasing number of FTs. During FTs, the migration of water and recrystallization of ice crystals caused by temperature fluctuations enhance gluten extrusion and intermolecular interactions of gluten, resulting in an uneven distribution of the electron cloud density of the S—S bonds, further compromising its bonding efficacy (Zhao et al., 2013). Partial cleavage of intermolecular disulfide bonds can cause gluten depolymerization (Zhang, Jia, Ma, Yang, Sun, & Li, 2022a). The water retention ability of sanxan can enhance the proportion of non-freezable water in SFFCNs and hinder the ability of the ice crystals to undergo recrystallization, thereby increasing the system's viscosity and mitigating the detrimental impact of ice crystals on S—S bonds destruction.

3.7. Effect of sanxan on the non-covalent interaction force of gluten in SFFCNs during FTs

In addition to the presence of S—S bonds, gluten structure and characteristics were influenced by non-covalent interactions, including ionic, hydrogen, and hydrophobic interactions (Li et al., 2019). The solubility of gluten in different solvents, as shown in Fig. 4, was used to assess the dynamic alterations of the intermolecular interactions between sanxan and gluten within SFFCNs during FTs. The solubility of the samples in S1and S2 was low, indicating that the ionic bond in SFFCNs gluten was weak (Wang, Zou, Tian, Gu, & Yang, 2018). The observed phenomenon could be attributed to the presence of amino acids that have side chains that could ionize at low concentrations. The low concentration of amino acids with ionizable side chains is responsible for the observed phenomenon. The observed phenomenon can be attributed to the low concentration of amino acids that possess ionizable side chains (Wieser, 2007). During FTs, the solubility of gluten in S1 and S2 in the control group increased by 6.60 % and 7.61 %, respectively. The solubility of the samples with sanxan increased by 6.25 % and 5.73 % in S1 and S2, respectively. This indicated that with the increase in the number of FTs, the organizational structure of gluten is disrupted by the expanding ice crystals, resulting in the deterioration of the secondary bonds responsible for maintaining the gluten structure. Alteration in the spatial configuration of wheat gluten could potentially result in an increase in small soluble molecular proteins, thereby enhancing solubility. Sanxan can significantly increase the solubility of gluten in S1 and S2, which may be due to the steric hindering effect of sanxan that can prevent the contact of ionizable amino acid residues on the molecular chain of gluten. As a result, the ionic interaction of gluten becomes weaker.

Gluten contains more hydrophilic groups and hydrophobic amino acids, and due to its unique amino acid composition, gluten contains a larger hydrophobic interaction region within the molecule and lower solubility. The solubility of the samples exhibited a significant increase

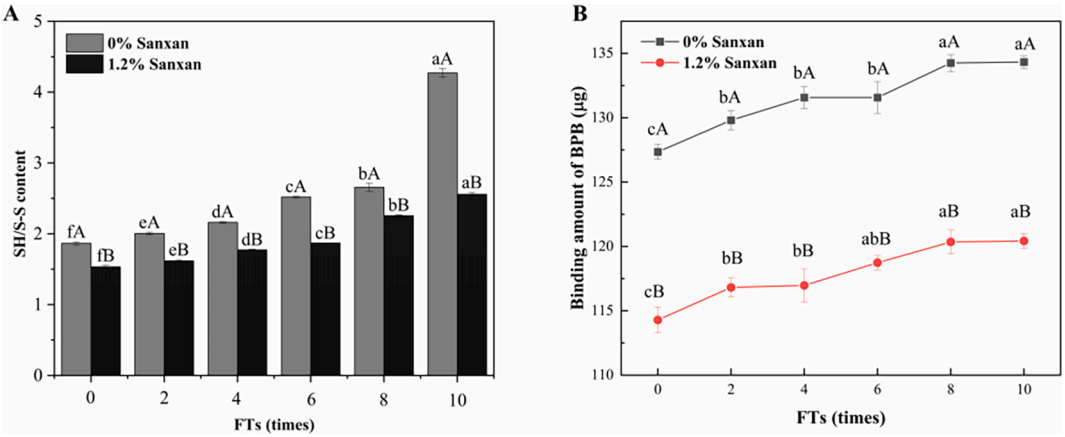

Fig. 3. (A) Effect of sanxan on the ratio of free sulfhydryl and disulfide bonds in gluten of SFFCNs during FTs; (B) Effect of sanxan on surface hydrophobicity of gluten of SFFCNs during FTs. Note: Different lowercase letters indicated significant difference under the same dosage and different FTs ($P < 0.05$); Different capital letters indicated that sanxan had significant differences under different dosage and same FTs ($P < 0.05$). Abbreviations are: SFFCNs, salt-free frozen-cooked noodles. FTs: freeze–thaw cycles.

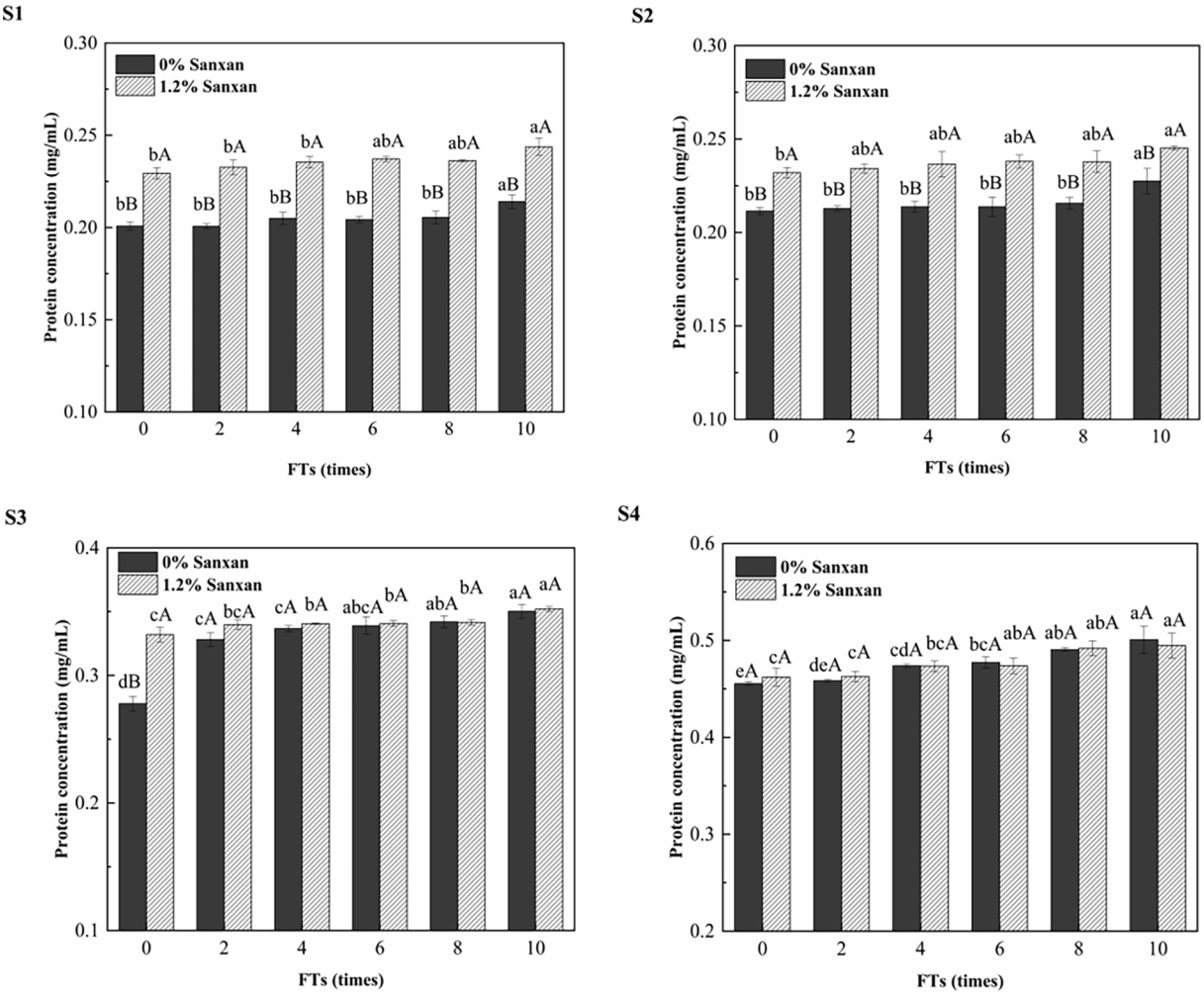

Fig. 4. Effect of sanxan on non-covalent bond interaction force of gluten of SFFCNs during FTs. Note: Different lowercase letters indicated significant difference under the same dosage and different FTs ($P < 0.05$); Different capital letters indicated that sanxan had significant differences under different dosage and same FTs ($P < 0.05$). Abbreviations are: SFFCNs, salt-free frozen-cooked noodles. FTs: freeze–thaw cycles.

when immersed in S3 and S4, since the presence of urea effectively disrupted the hydrogen bonding and hydrophobic interactions, thus facilitating gluten dissolution within the solvent (Si et al., 2021). The urea concentration in the S4 solution was much higher than that in the S3 solution, so the non-covalent interactions between gluten molecules were completely disrupted and the solubility of the samples in the S4

solution was further increased. The solubility of the control group in S3 and S4 increased by 26.02 % and 9.94 % before and after freeze-thawing, respectively, while the samples with the addition of sanxan increased by 6.08 % and 7.07 %, respectively. This indicates that the freeze–thaw stability of sanxan plays a crucial role in minimizing the damage caused by ice crystals to the structure of the gluten network during FTs, restricting the extent of dissociation in gluten side chains and consequently decreasing solubility. On the other hand, the presence of sanxan can enhance the hydrophobic interactions of gluten, so that the gluten maintains a relatively stable spatial structure and reduces the mechanical damage to the gluten network induced by ice crystals, thus exhibiting a lower solubility. Therefore, the hydrogen bond changes of gluten in SFFCNs under the action of sanxan are consistent with those of the 3.5 mirco-environment of aromatic amino acids.

3.8. Effect of sanxan on the surface hydrophobicity of gluten in SFFCNs during FTs

Surface hydrophobicity serves as an indicator of the ability of protein molecules to interact with each other, which significantly influences the extent of protein molecule aggregation and solubility (Wagner, Sorgentini, & Anon, 2000). The solubility of the protein was influenced by the interaction between its hydrophilic and hydrophobic characteristics, along with the spatial arrangement of amino acids on its surface (Moure, Sineiro, Domínguez, & Parajó, 2006).The rearrangement of hydrophobic components from the molecular surface to the hydrophobic region results in modifications in amino acid composition, leading to a decrease in interaction with water molecules, an increase in hydrophobicity, and a reduction in protein solubility (Jiang et al., 2015).

There was a positive correlation between the amount of BPB binding and the number of FTs. As shown in Fig. 3B, BPB binding increased by 7.84 % (from 127.34 to 134.33 μg) before and after FTs in the control group and by 5.37 % (from 114.29 to 120.43 μg) in the experimental group. During FTs, the volume of ice crystals in the SFFCNs system expands with temperature fluctuations, which changes the conformation of gluten. At the same time, because of the weaker interaction between proteins, some proteins unfolded, leading to an increase in the exposure of hydrophobic regions previously concealed within the molecules. Consequently, this resulted in an increase in the hydrophobic surface of the proteins.

In contrast to the control group, the experimental group demonstrated a decrease in BPB binding, suggesting that the gluten's hydrophobic sites were shielded, resulting in a reduced surface hydrophobicity. Tang et al. (2019) observed a decrease in the surface hydrophobicity of gluten after incorporation of carboxymethyl cellulose (CMC). Kato and Nakai (1980) used hydrophobic partitioning to evaluate the surface hydrophobic characteristics of native, unfolded and surfactant-bound proteins. The findings indicated an inverse relationship between the α-helix content of the proteins and their surface hydrophobicity. Other studies have also demonstrated a significant direct relationship between the content of random coil formations and the level of hydrophobicity exhibited on their surfaces (Jiang et al., 2015). Therefore, the sanxan-induced alterations in the gluten surface hydrophobicity of the SFFCNs exhibited a similar trend to the variations observed in α-helix and the random coil composition within the 3.3 secondary structure.

4. Conclusions

In this study, the compositional and structural properties of gluten in SFFCNs with a proper amount of sanxan were investigated as FTs increased. The action mechanism of sanxan on gluten was elucidated in terms of the molecular weight distribution and subunit distribution, covalent and non-covalent bonds, secondary structure, conformation of S—S bonds bridge, micro-environment of amino acids, and surface hydrophobicity. The results showed that sanxan had the ability to regulate the molecular weight distribution and subunit composition of gluten. Additionally, the addition of 1.2 % sanxan increased the total amount of glutenin and decreased the total amount of gliadin, thereby promoting gluten aggregation compared to the control group. Analysis of the protein conformation showed that after 10 FTs, the content of α-helices in the control group decreased rapidly from 15.45 % to 10.74 %, while the content of random coils increased significantly from 19.19 % to 26.53 %. In contrast, the sanxan with 1.2 % addition only changed by 1.13 % and 1.04 %, respectively, indicating that sanxan was able to enhance the freeze–thaw stability of SFFCNs. In addition, the presence of sanxan retarded the breakage of the S—S bonds and contributed to an increase in the percentage of g-g-g structure in the S—S bonds bridge (3.96 %). In conclusion, the addition of sanxan increased the viscosity of the system and decreased the phase transition in water, thereby delaying changes in molecular weight, conformation, and protein interactions of SFFCNs during FTs. These results elucidated the mechanism by which sanxan enhances the quality of SFFCNs from the perspective of gluten. In addition, it is necessary to investigate the interaction between sanxan and starch in SFFCNs during frozen storage and cooking in order to fully explore the mechanism of improvement.

CRediT authorship contribution statement

Ying Liang: Conceptualization, Methodology, Supervision, Writing – original draft. **Xiuling Zhu:** Conceptualization, Formal analysis, Writing – review & editing. **Hao Liu:** Data curation, Software. **Jiayi Wang:** Investigation, Validation. **Baoshan He:** Resources, Validation. **Jinshui Wang:** Funding acquisition, Project administration, Supervision.

Declaration of competing interest

The authors declare that they have no known competing financial interests or personal relationships that could have appeared to influence the work reported in this paper.

Data availability

Data will be made available on request.

Acknowledgments

This work was supported by the Joint Fund of Science and Technology Research and Development Plan of Henan Province in 2022 (225200810110); Scientific and Collaborative Innovation Special Project of Zhengzhou, Henan Province (21ZZXTCX03); For youth backbone teachers in colleges and universities of Henan province funded (2023GGJS061); Special Funds to Subsidize Scientific Research Projects in Zhengzhou R&D (22ZZRDZX34); the open project program of the National Engineering Research Center of Wheat and Corn Further Processing, Henan University of Technology (NL2022016); The "Double First-Class" Project for Postgraduate-Cultivating Innovation Platform Establishment Programme of Henan University of Technology (HAUTSYL2023PT04).

Appendix A. Supplementary data

Supplementary data to this article can be found online at https://doi.org/10.1016/j.fochx.2024.101229.

References

Aghagholizadeh, R., Kadivar, M., Nazari, M., Mousavi, F., Azizi, M. H., Zahedi, M., et al. (2017). Characterization of wheat gluten subunits by liquid chromatography - Mass spectrometry and their relationship to technological quality of wheat. *Journal of Cereal Science, 76*, 229–235. https://doi.org/10.1016/j.jcs.2017.06.016

Badii, F., & Howell, N. (2006). Fish gelatin: Structure, gelling properties and interaction with egg albumen proteins. *Food Hydrocolloids, 20*(5), 630–640. https://doi.org/10.1016/j.foodhyd.2005.06.006

Brandt, N. N., Chikishev, A. Y., Golovin, A. V., Kruzhilin, V. N., & Zalevsky, A. O. (2014). Raman spectroscopy of disulfide bridges in thrombin. *Biomedical Spectroscopy and Imaging, 3*(3), 287–292. https://doi.org/10.3233/bsi-140081

Chen, G. J., Hu, R. J., & Li, Y. H. (2018). Potassium chloride affects gluten microstructures and dough characteristics similarly as sodium chloride. *Journal of Cereal Science, 82*, 155–163. https://doi.org/10.1016/j.jcs.2018.06.008

Georget, D. M. R., & Belton, P. S. (2006). Effects of temperature and water content on the secondary structure of wheat gluten studied by FTIR spectroscopy. *Biomacromolecules, 7*(2), 469–475. https://doi.org/10.1021/bm050667j

Hong, T., Ma, Y., Yuan, Y., Guo, L., Xu, D., Wu, F., et al. (2021). Understanding the influence of pullulan on the quality changes, water mobility, structural properties and thermal properties of frozen cooked noodles. *Food Chemistry, 365*, Article 130512. https://doi.org/10.1016/j.foodchem.2021.130512

Jiang, L. Z., Wang, Z. J., Li, Y., Meng, X. H., Sui, X. N., Qi, B. K., et al. (2015). Relationship between surface hydrophobicity and structure of soy protein isolate subjected to different ionic strength. *International Journal of Food Properties, 18*(5), 1059–1074. https://doi.org/10.1080/10942912.2013.865057

Kato, A., & Nakai, S. (1980). Hydrophobicity determined by a fluorescence probe method and its correlation with surface properties of proteins. *Biochimica et Biophysica Acta, 624*(1), 13–20. https://doi.org/10.1016/0005-2795(80)90220-2

Li, C. F., Chen, G. J., Ran, C. X., Liu, L. J., Wang, S. S., Xu, Y., et al. (2019). Adlay starch-gluten composite gel: Effects of adlay starch on rheological and structural properties of gluten gel to molecular and physico-chemical characteristics. *Food Chemistry, 289*, 121–129. https://doi.org/10.1016/j.foodchem.2019.03.030

Li, M., Sun, Q. J., Han, C. W., Chen, H. H., & Tang, W. T. (2018). Comparative study of the quality characteristics of fresh noodles with regular salt and alkali and the underlying mechanisms. *Food Chemistry, 246*, 335–342. https://doi.org/10.1016/j.foodchem.2017.11.020

Li, J., Sun, L., Li, B. L., Liu, M., Liang, Y., Ma, H., et al. (2022). Evaluation on the water state of frozen dough and quality of steamed bread with proper amount of sanxan added during freeze-thawed cycles. *Journal of Cereal Science, 108*, Article 103564. https://doi.org/10.1016/j.jcs.2022.103564

Liang, Y., Song, J. Y., Chen, Z. L., Liu, M., Chen, S. H., Liu, H., et al. (2023). Influence of sanxan on the quality of salt-free frozen-cooked wheat noodles during freeze-thaw cycles. *International Journal of Food Science & Technology, 58*(2), 574–585. https://doi.org/10.1111/ijfs.16201

Liang, Y., Chen, Z. L., Liu, M., Qu, Z. T., Liu, H., Song, J. Y., et al. (2022). Effect of curdlan on the aggregation behavior and structure of gluten in frozen-cooked noodles during frozen storage. *International Journal of Biological Macromolecules, 205*, 274–282. https://doi.org/10.1016/j.ijbiomac.2022.02.085

Liang, Y., Qu, Z. T., Liu, M., Wang, J. S., Zhu, M. F., Liu, Z. L., et al. (2020). Effect of curdlan on the quality of frozen-cooked noodles during frozen storage. *Journal of Cereal Science, 95*, Article 103019. https://doi.org/10.1016/j.jcs.2020.103019

Liu, H., Liang, Y., Zhang, S. Y., Liu, M., He, B. S., Wu, X. Q., et al. (2024). Physicochemical properties and conformational structures of pre-cooked wheat gluten during freeze-thaw cycles affected by curdlan. *Food Hydrocolloids, 147*, Article 109381. https://doi.org/10.1016/j.foodhyd.2023.109381

Moure, A., Sineiro, J., Domínguez, H., & Parajó, J. C. (2006). Functionality of oilseed protein products: A review. *Food Research International, 39*(9), 945–963. https://doi.org/10.1016/j.foodres.2006.07.002

Nawrocka, A., Szymanska-Chargot, M., Mis, A., Ptaszynska, A. A., Kowalski, R., Wasko, P., et al. (2015). Influence of dietary fibre on gluten proteins structure - a study on model flour with application of FT-Raman spectroscopy. *Journal of Raman Spectroscopy, 46*(3), 309–316. https://doi.org/10.1002/jrs.4648

Obadi, M., Zhang, J. Y., Shi, Y. N., & Xu, B. (2021). Factors affecting frozen cooked noodle quality: A review. *Trends in Food Science & Technology, 109*, 662–673. https://doi.org/10.1016/j.tifs.2021.01.033

Pan, Z. L., Ai, Z. L., Wang, T., Wang, Y. H., & Zhang, X. L. (2016). Effect of hydrocolloids on the energy consumption and quality of frozen noodles. *Journal of Food Science and Technology-Mysore, 53*(5), 2414–2421. https://doi.org/10.1007/s13197-016-2217-9

Reissner, A. M., Wendt, J., Zahn, S., & Rohm, H. (2019). Sodium-chloride reduction by substitution with potassium, calcium and magnesium salts in wheat bread. *Lwt-Food Science and Technology, 108*, 153–159. https://doi.org/10.1016/j.lwt.2019.03.069

Si, X. J., Li, T. T., Zhang, Y., Zhang, W. H., Qian, H. F., Li, Y., et al. (2021). Interactions between gluten and water-unextractable arabinoxylan during the thermal treatment. *Food Chemistry, 345*, Article 28785. https://doi.org/10.1016/j.foodchem.2020.128785

Tang, Y., Yang, Y. X., Wang, Q. M., Tang, Y. W., Li, F. H., Zhao, J. C., et al. (2019). Combined effect of carboxymethylcellulose and salt on structural properties of wheat gluten proteins. *Food Hydrocolloids, 97*, Article 105189. https://doi.org/10.1016/j.foodhyd.2019.105189

Ukai, T., Matsumura, Y., & Urade, R. (2008). Disaggregation and reaggregation of gluten proteins by sodium chloride. *Journal of Agricultural and Food Chemistry, 56*(3), 1122–1130. https://doi.org/10.1021/jf0725676

Wagner, J. R., Sorgentini, D. A., & Anon, M. C. (2000). Relation between solubility and surface hydrophobicity as an indicator of modifications during preparation processes of commercial and laboratory-prepared soy protein isolates. *Journal of Agricultural and Food Chemistry, 48*(8), 3159–3165. https://doi.org/10.1021/jf990823b

Wang, K. Q., Luo, S. Z., Zhong, X. Y., Cai, J., Jiang, S. T., & Zheng, Z. (2017). Changes in chemical interactions and protein conformation during heat-induced wheat gluten gel formation. *Food Chemistry, 214*, 393–399. https://doi.org/10.1016/j.foodchem.2016.07.037

Wang, P., Chen, H. Y., Mohanad, B., Xu, L., Ning, Y. W., Xu, J., et al. (2014). Effect of frozen storage on physico-chemistry of wheat gluten proteins: Studies on gluten-, glutenin- and gliadin-rich fractions. *Food Hydrocolloids, 39*, 187–194. https://doi.org/10.1016/j.foodhyd.2014.01.009

Wang, P., Wu, F. F., Rasoamandrary, N., Jin, Z. Y., & Xu, X. M. (2015). Frozen-induced depolymerization of glutenin macropolymers: Effect of the frozen storage time and gliadin content. *Journal of Cereal Science, 62*, 159–162. https://doi.org/10.1016/j.jcs.2015.01.005

Wang, P., Zou, M., Li, D. D., Zhou, Y. L., Jiang, D., Yang, R. Q., et al. (2020). Conformational rearrangement and polymerization behavior of frozen-stored gluten during thermal treatment. *Food Hydrocolloids, 101*, Article 105502. https://doi.org/10.1016/j.foodhyd.2019.105502

Wang, P., Zou, M., Tian, M. Q., Gu, Z. X., & Yang, R. Q. (2018). The impact of heating on the unfolding and polymerization process of frozen-stored gluten. *Food Hydrocolloids, 85*, 195–203. https://doi.org/10.1016/j.foodhyd.2018.07.019

Wang, X. H., Liang, Y., Wang, Q., Zhang, X., & Wang, J. S. (2021). Effect of low-sodium salt on the physicochemical and rheological properties of wheat flour doughs and their respective gluten. *Journal of Cereal Science, 102*, Article 103371. https://doi.org/10.1016/j.jcs.2021.103371

Wang, X. Y., Guo, X. N., & Zhu, K. X. (2016). Polymerization of wheat gluten and the changes of glutenin macropolymer (GMP) during the production of Chinese steamed bread. *Food Chemistry, 201*, 275–283. https://doi.org/10.1016/j.foodchem.2016.01.072

Wang, Y. H., Zhang, Y. R., Xu, F., & Li, Z. K. (2020). Effects of water addition and noodle thickness on the surface tackiness of frozen cooked noodles. *Journal of Food Processing and Preservation, 44*(9), 11. https://doi.org/10.1111/jfpp.14717

Wieser, H. (2007). Chemistry of gluten proteins. *Food Microbiology, 24*(2), 115–119. https://doi.org/10.1016/j.fm.2006.07.004

Wieser, H., Antes, S., & Seilmeier, W. (1998). Quantitative determination of gluten protein types in wheat flour by reversed-phase high-performance liquid chromatography. *Cereal Chemistry, 75*(5), 644–650. https://doi.org/10.1094/cchem.1998.75.5.644

Wu, M. M., Shi, Z., Huang, H. D., Qu, J. M., Dai, X. H., Tian, X. F., et al. (2017). Network structure and functional properties of transparent hydrogel sanxan produced by Sphingomonas sanxanigenens NX02. *Carbohydrate Polymers, 176*, 65–74. https://doi.org/10.1016/j.carbpol.2017.08.057

Zhang, M. L., Jia, R. B., Ma, M., Yang, T. B., Sun, Q. J., & Li, M. (2022a). Versatile wheat gluten: Functional properties and application in the food-related industry. *Critical Reviews in Food Science and Nutrition, 63*(30), 11–17. https://doi.org/10.1080/10408398.2022.2078785

Zhang, M. L., Ma, M., Yang, T. B., Li, M., & Sun, Q. J. (2022b). Dynamic distribution and transition of gluten proteins during noodle processing. *Food Hydrocolloids, 123*, 11. https://doi.org/10.1016/j.foodhyd.2021.107114

Zhao, L., Li, L., Liu, G. Q., Chen, L., Liu, X. X., Zhu, J., et al. (2013). Effect of freeze-thaw cycles on the molecular weight and size distribution of gluten. *Food Research International, 53*(1), 409–416. https://doi.org/10.1016/j.foodres.2013.04.013

Zhou, Y., Zhao, D., Foster, T. J., Liu, Y. X., Wang, Y., Nirasawa, S., et al. (2014). Konjac glucomannan-induced changes in thiol/disulphide exchange and gluten conformation upon dough mixing. *Food Chemistry, 150*, 164–165. https://doi.org/10.1016/j.foodchem.2013.11.001